FAST ASSESSMENT OF RF POWER ABSORPTION IN INDOOR ENVIRONMENTS BY ROOM ELECTROMAGNETICS THEORY

Aliou Bamba[1], Wout, Joseph[1], Achilles Boursianis[2], Theodoros Samaras[2], Günter Vermeeren[1], Arno Thielens[1], and Luc, Martens[1]

(email:wout.joseph@intec.UGent.be, tel : +32 9 33 14918, fax:+32 9 33 14899)

[1]Department of Information Technology, Ghent University / iMinds

Gaston Crommenlaan 8, B-9050 Ghent, Belgium

[2]Radiocommunications Laboratory, Department of Physics, Aristotle University of Thessaloniki, GR-54124 Thessaloniki, Greece

Abstract- **A fast method to assess radiofrequency (RF) radiation absorption in humans present in realistic indoor environments is proposed. The only required inputs are the room characteristics and the weight and position of the human with respect to the electromagnetic source. The method is compared and validated with full FDTD simulations. Various realistic scenarios are investigated, in which one to six human phantoms are present. Whole-body power absorption ranges from 23.5 to 85.9 µW/kg with a median deviation of about 3.1 dB (51%). While this difference may appear large, it is outbalanced by a calculation time of less than a second for the proposed method compared to about 17.5 hours for a single single full-wave electromagnetic simulation.**

***Key Words*- whole-body absorption; indoor; room electromagnetics; exposure**

I. INTRODUCTION

People spend most of their time indoors, i.e., at home, in offices, schools, etc.[(1)] Adults (30-59 years old) and young people (15-29 years old) spend 83% and 93% of their time indoor, at daytime (8am-6pm) and night (6pm – 8am), respectively. More and more wireless technologies such as smartphones and tablets are being used, accessing the wireless local area (WLAN) networks using WiFi technology or indoor femtocells using cellular LTE (Long Term Evolution) technology. This rapid expansion of wireless devices and networks in indoor environments causes an increase of human exposure to radiofrequency (RF) radiation[(2)]. Moreover, the electromagnetic fields (EMF) exposure and distribution in indoor environments is very diverse, also when comparing different countries[(3)]. Some of these environments such as schools and homes are considered as sensitive, since children are often present in them. WHO[(4)] emphasized the need to characterize RF electromagnetic field (RF-EMF) emissions and assess exposure levels for new and emerging RF technologies, such as LTE and the newest WLAN protocols (802.11ac etc).

The characterization of indoor exposure and RF power absorption in humans is a difficult task. Measurement campaigns in indoor environments are time-consuming and provide only a limited set of electromagnetic data and not the actual absorption[5, 6, 2]. Only Refs. (7, 8) and Ref. (9) proposed a measurement method for indoor absorption and absorption cross section (ACS) in real environments, but this method is also time-consuming and expensive measurement equipment has to be used. The whole-body specific absorption rate (SAR) can also be determined from personal exposimeter data[10,11]. As an alternative, full-wave electromagnetic simulations can be performed. However, these are very difficult as the full indoor environment has to be modelled in detail; therefore, high performance computing (HPC), e.g., employing GPU clusters, is required to obtain results within a reasonable time of hours or days[12].

Moreover, the radio channel not only consists of specular paths with well-defined *discrete* locations in the different radio channel dimensions (e.g., space, frequency, time, etc.) but also of diffuse or dense multipath components (DMC), which are *continuous* across these dimensions and present in the room, due to the non-coherent reflections off scatterers. It has been shown that the DMC power density may contribute significantly in indoor environments (up to 95%)[7]. Using the new modelling approach, based upon the *room electromagnetics (REM)* approach[9], it will be possible to estimate in a fast way the human absorption and ACS in indoor environments. Basically, the theory states that the Power Delay Profile (PDP) of indoor environments is comprised of two parts: the Line-Of-Sight (LOS) signal, if any, and the diffuse fields.

Our goal is to assess very fast the whole-body absorption in humans present in real indoor environments, only knowing the room characteristics and the weight and position of the human with respect to the electromagnetic source (access point or femtocell). To realize this, we propose the room electromagnetics method and we validate the proposed method with Finite-Difference Time-Domain (FDTD) simulations.

II. MATERIALS AND METHOD

A. Configuration

The following scenarios are considered. In a realistic model of a teleconference classroom (7.47 m × 5.96 m × 3.1 m) at the Aristotle University of Thessaloniki in Greece, a half-wavelength dipole transmitter (Tx) antenna at 2.75 GHz (representative for LTE at 2.6 GHz and WLANs around 2.4 GHz) was placed at point Tx (Figure 1). This enabled also validation measurements [Mouhtaropoulos et al., 2013]. Fifteen scenarios were simulated with the room containing 1 human model, 3, and 6 human models. Two phantoms of the virtual family were considered, the adult male Duke and adult female Ella[13]. The 15 scenarios are listed in Table 1, with indication of the phantoms (1, 3 and 6) and their locations. Figure 1 shows the FDTD model (Figure 1 (a)) and a picture of the classroom (Figure 1 (c)), with the positions of the phantoms in the classroom (Figure 1 (b)) as listed in Table 1.

B. FDTD simulations

The FDTD calculations were performed with SEMCAD-X (Schmid and Partner Engineering AG, Zurich, Switzerland). The model consisted of walls, desks, chairs, etc., of the realistic indoor environment with their actual dimensions. The Tx antenna was modeled as an edge source of 1 V/m amplitude, corresponding to an input power of 14.1 mW. However, all the results were normalized to 1 W. The frequency of the harmonic simulation was set to 2.75 GHz, while the simulation time was 500 periods. A grid resolution of 1 cm was selected (although not optimal for the frequency in the presence of human tissues), resulting in approximately 317.5 million voxels in the computational domain. All metallic objects were assumed as perfectly electric conductors. The simulation was carried out using four GPU Tesla T10 accelerators with total memory of 16,380 MBytes (4,095 MBytes each) in a CentOS release 5.5 Linux workstation with 2 x Dual

Core AMD Opteron Central Processor Units at 2400 MHz and 16 GBytes of RAM. The total simulation time of a single scenario was 17.5 h.

C. Room electromagnetics method

Figure 2 shows a flow-graph of the proposed method based upon the REM technique and the comparison with full-wave FDTD calculations. The input parameters have been described above and consist of the room characteristics, the electromagnetic source, and the phantoms and their positions in the room.

First, for our proposed method, we start with the determination of the incident power densities due to the LOS specular fields S_{los} and due to the diffuse fields S_{dmc} [7,8]

$$S_{los} = \frac{P_0}{4\pi d_0^2} \text{ (W/m}^2\text{)}; \; S_{dmc} = \frac{c_0 \tau P_0}{4\pi V} e^{-\frac{d_0}{c_0 \tau}} . \eta_{pol} \text{ (W/m}^2\text{)} \quad (1)$$

where P_0, d_0, τ, and η_{pol} are the transmitted power, the distance Tx-phantom, the reverberation time, and the polarization factor of diffuse fields, respectively. We consider here $\eta_{pol} = 0.5$, corresponding to a polarization angle of 45° [9], because we assume complete depolarization. Further, V, $c_0 = 3\times10^8$ m/s, and τ are the room volume (138 m^3 here), the velocity of light in vacuum, and the reverberation time, respectively. The power density S_{dmc} of the diffuse component can thus be important indoor.

Second, the reverberation time τ (second box in the REM part of Figure 2) of the investigated empty room (i.e., without humans), which is the decay rate of the diffuse power in an indoor environment and describes all the losses in a complex indoor environment, is determined using Ref. (14) (eq. 10):

$$\tau = \frac{V(0.473 f^3 - 24.9 f^2 + 321 f - 254}{2\pi f A} \text{ (s)} \quad (2)$$

With *f* the frequency under consideration (here 2.75 GHz) and A the total area of the room (including the floor, walls, ceiling, and objects). For the considered configuration and room, we obtain a reverberation time of 20.87 ns. Thus, with only inputs the room characteristics (volume,

area), the frequency, and the separation from the source we are able to calculate the reverberation time τ of the room and the resulting specular LOS and diffuse incident power densities.

Third, as mentioned above, we determine now the total whole-body specific absorption rate (SAR_{tot}), using the REM theory in Figure 2, as the sum of the SAR due to the LOS specular fields SAR_{los} and the SAR due to the diffuse fields SAR_{dmc}. From the room electromagnetics theory in Ref. (8) (eq. 13 and 14) we obtain the total whole-body SAR_{tot} as follows:

$$SAR_{tot} = SAR_{los} + SAR_{dmc} = 0.21 \cdot m^{-0.3534} \cdot \eta \cdot S_{tot}(\alpha + k(1-\alpha)) \text{ (W/kg)} \qquad (3)$$

where m the mass (larger or equal to 10 kg, 72.4 kg for the adult man Duke and 58.7 kg for the adult female Ella), k the ratio between the absorption cross section (ACS) for LOS fields ACS_{los} and the absorption cross section for diffuse fields ACS_{dmc} (diffuse multipath components or DMC), η the ratio between the ACS_{dmc} and the total projected body surface area, and S_{tot} the total power density (sum of S_{los} and S_{dmc} of eq. (1)); α in eq. (3) is the diffuse percentage S_{dmc}/S_{tot} calculated from eq. (1), i.e., the ratio of the power density in diffuse fields and the total power density. For the considered environment α varies from 8% (position 9 near the source) to 26% (positions further from the source, e.g., 26-27-28). It is clear that near the antenna Tx the diffuse fields are not dominating (lower ratio α of the diffuse percentage) but further from the Tx, DMC power density becomes more important with respect to the LOS component power density (higher α). The ratio η is determined as $\eta = -1.7827 \cdot 10^{-5} \cdot f + 0.5859$ (f in MHz, eq. (8) of Ref. (8)). For k, the average value is considered, i.e., for an azimuth of 45º, k = 0.145[8].

In summary, the room characteristics and position of phantom in the room (eq. (1) and (2)) and the phantom's weight (eq. (3)) enable to estimate the whole-body SAR of a phantom or person in a room. These calculations only take seconds compared to the FDTD simulations of several hours.

III. RESULTS AND DISCUSSION

Figure 3 shows a bar plot of the calculated whole-body SAR using the REM theory and the SAR obtained using the FDTD simulations for the all considered positions. The error bars were calculated from the uncertainties of the FDTD simulations[15,16]. Positions closer to the source cause highest whole-body absorptions due to the LOS fields. Highest absorptions occur in the female model (Ella) because of her lower weight than the male model. A good/acceptable agreement can be noticed. The median deviation for Duke and Ella for all positions and scenarios is 3.5 dB (54%), and 2.7 dB (46%), respectively. Maximum deviations up to 5 dB (factor 3) are possible. Deviations between the two methods are expected anyway, due to the fact that shadowing of the phantoms (when multiple models are present at the same time in the room) is not accounted for in the REM theory and furniture is also neglected. Moreover, the considered room is relatively small, even though it requires a huge effort to calculate with FDTD; therefore, the contribution of the diffuse part is not as important as for larger rooms, which would result in better agreement as the DMC will dominate for larger separations from the source. This indicates that the REM method is a very useful method to estimate very fast real-life whole body absorptions.

The maximum whole-body SAR for all scenarios and positions was 85.9 µW/kg (mean value of 23.5 µW/kg), thus all values satisfy the ICNIRP basic restriction of 0.08 W/kg for the general public[17] for a CW (continuous wave) transmission power of 1 W from the antenna. Table 1 and Figure 4 compare the average SAR_{wb} over all humans for each scenario. The REM theory overestimates the absorption in comparison to the FDTD simulations. An explanation is that the roughness of the surfaces (walls, floor, ceiling, etc.) is not modeled in the FDTD simulation. Therefore, the contribution of the DMC in the FDTD simulations is smaller than in the REM method. Nevertheless, the fact that higher values of whole-body SAR (overestimations compared

to FDTD) are calculated by the REM method is beneficial in terms of safety assessment, since it means that this is a *conservative method*, which presents a worst-case approach.

The median and maximal deviation for the average SAR_{wb} for all scenarios (FDTD versus REM) is 3.1 dB (51%) and 4.3 dB (62 %), respectively, which is acceptable to have an estimate about actual absorptions in real environments without time-intensive computations or measurement campaigns, which have uncertainties for the electric field of ± 3 dB (CENELEC[18]).

IV. CONCLUSIONS

In general, one can conclude that the proposed theory is a valid alternative for time-consuming simulations or measurements, in order to assess the whole-body absorption in real indoor environments. Only room geometrical features and the weight and position of the human with respect to the electromagnetic source are the required inputs. Future work will consist of extending the theory to considering shadowing due to other present phantoms, accounting for multiple sources within a room, and studying various rooms with different characteristics and different phantoms present. Furthermore, the REM theory will be applied on measurement data of personal exposimeters in indoor environments in order to enable these exposimeters to measure diffuse fields, which can dominate indoor environments, instead of only accounting for specular fields, as currently is done. Finally, other numerical techniques, like radiosity combined with specular reflections, which is less computationally intensive than FDTD, will be implemented for power absorption calculations.

REFERENCES

1. Aliaga, C. *How is the time of women and men distributed in Europe. Statistics in focus, population and social conditions*. ISSN 1024-4352, KS-NK-06-004-EN-N, Eurostat Luxembourg**.** Available at

http://www.unece.org/fileadmin/DAM/stats/gender/timeuse/DataReports/How_is_the_time_of_Women_and_Men.pdf, (2006), Last Accessed July 6 2015.

2. Verloock, L., Joseph, W., Goeminne, F., Martens, L., Verlaek, M., and Constandt, K. *Assessment of radio frequency exposures in schools, homes, and public places in Belgium*. Health Physics 107(6), 503-513 (2014).
3. Joseph, W., Frei, P., Roösli, M., Thuróczy, G., Gajsek, P., Trcek, T., Bolte, J., Vermeeren, G., Mohler, E., Juhasz, P., Finta, V., Martens, L. *Comparison of personal radio frequency electromagnetic field exposure in different urban areas across Europe*. Environmental Research 110, 658 – 663 (2010).
4. World Health Organization (WHO). *Radio frequency (RF) fields research agenda*. Available at http://www.who.int/peh-emf/research/agenda/en/index.html, Last Accessed September 3, 2015.
5. Tomitsch, J., Dechant, E., and Frank, W. *Survey of Electromagnetic Field Exposure in Bedrooms of Residences in Lower Austria*. Bioelectromagnetics 31, 200-208 (2010).
6. Verloock, L., Joseph, W., Vermeeren, G., and Martens, L. *Procedure for assessment of general public exposure from WLAN in offices and in wireless sensor network testbed*. Health Physics 98(4), 628-638 (2010).
7. Bamba, A., Joseph, W., Vermereen, G., Tanghe, E., Gaillot, D. P., Andersen, J. B., Nielsen, J., Lienard, M., Martens, L. *Validation of Experimental Whole-body SAR Assessment Method in a Complex Environment*. Bioelectromagnetics 34, 122-132 (2013).
8. Bamba, A., Joseph, W., Vermeeren, G., Thielens, A., Tanghe, E., Martens, L. *A Formula for Human Average Whole-Body SAR_{wb} under Diffuse Fields Exposure in the GHz region*. Physics in Medicine and Biology 59(23), 7435-7456 (2014).
9. Andersen, J.B., Nielsen, J.O., Pedersen, G.F., Bauch, G., and Herdin, M. *Room Electromagnetics*. IEEE Antennas and propagation Magazine 49 (2), 27-33 (2007).

10. Joseph, W., Vermeeren, G., Verloock, L., Martens, L. *Estimation of whole-body SAR from electromagnetic fields using personal exposure meters*. Bioelectromagnetics 31(4), 286-295 (2010).

11. Thielens, A., Vanveerdeghem, P., Agneessens, S., Van Torre, P., Vermeeren, G., Rogier, H., Martens, L., Joseph, W. *Whole-Body Averaged Specific Absorption Rate Estimation using a Personal, Distributed Exposimeter*. IEEE Antennas and Wireless Propagation Letters AWPL 14, 1534 - 1537 doi: 10.1109/LAWP.2014.2368597 (2014).

12. Mouhtaropoulos, D., Boursianis, A., and Samaras, T. *Prediction of transmission path loss in indoor environments with the radiosity method*. Microwave and optical technology letters 55, 2401-2405 (2013).

13. Christ, A., Kainz, W., Hahn, E., Honegger, K., Zefferer, M., Neufeld, E., Rascher, W., Janka, R., Bautz, W., Chen, J., Kiefer, B., Schmitt, P., Hollenbach, H. P., Shen, J., Oberle, M., Szczerba, D., Kam, A., Guag, J., Kuster N. *The Virtual Family - Development of Surface-Based Anatomical Models of Two Adults and Two Children for Dosimetric Simulations*. Physics in Medicine and Biology 55(2), N23-N38 (2010).

14. Bamba, A., Martinez-Ingles, M-T., Gaillot, D. P., Tanghe, E., Hanssens, B., Molina-Garcia-Pardo, J-M., Lienard, M., Martens, L., Joseph, W.. *Experimental Investigation of Electromagnetic Reverberation Characteristics as a function of UWB Frequencies*. IEEE Antennas and Wireless Propagation Letters 14, 859 – 862 (2015).

15. Bakker, J.F., Paulides, M.M., Christ, A., Kuster, N., van Rhoon, G.C. *Assessment of induced SAR in children exposed to electromagnetic plane waves between 10 MHz and 5.6 GHz*. Phys Med Biol 55, 3115-3130 (2010).

16. Bakker, J.F., Paulides, M.M., Christ, A., Kuster, N., van Rhoon, G.C. *Corrigendum for assessment of induced SAR in children exposed to electromagnetic plane waves between 10 MHz and 5.6 GHz*. Phys Med Biol 56, 2883 (2011).

17. International Commission on Non-ionizing Radiation Protection (ICNIRP). *Guidelines for limiting exposure to time-varying electric, magnetic, and electromagnetic fields (up to 300 GHz)*. Health Phys 74(4), 494–522 (1998).
18. CENELEC European Committee for Electrotechnical Standardisation TC 106x WG1 EN 50492 in situ. *Basic standard for the in-situ measurement of electromagnetic field strength related to human exposure in the vicinity of base stations*; 2008.

Author affiliations

Aliou Bamba[1], Wout, Joseph[1], Günter Vermeeren[1], Arno Thielens[1], and Luc, Martens[1]

[1]Department of Information Technology, Ghent University / iMinds,

Gaston Crommenlaan 8, box 201, B-9050 Ghent, Belgium, fax: +32 9 33 14899

(email:wout.joseph@intec.UGent.be)

Achilles Boursianis[2], Theodoros Samaras[2],

[2]Radiocommunications Laboratory, Department of Physics, Aristotle University of Thessaloniki, GR-54124 Thessaloniki, Greece

(email: theosama@auth.gr)

Acknowledgement: The research leading to these results has received funding from the European Union's Seventh Framework Programme project SEAWIND under grant agreement no 244149.

List of captions

TABLE 1: The considered scenarios, present human models, and comparison of the indoor average whole-body SAR (W/kg) obtained from the FDTD simulations and REM calculations.

Figure 1: (a) Perspective view of the realistic model (teleconference classroom) with six phantoms, (b) Top view of the realistic model (the possible positions where phantoms have been placed are indicated with numbers, as well as the position of the Tx antenna) and (c) Photo of the teleconference classroom.

Figure 2: Flow graph of the proposed REM method and comparison with full-wave FDTD calculations.

Figure 3: Comparison of whole-body SAR values obtained using the fast REM method and the FDTD simulations, for the different positions within the room.

Figure 4: Comparison of average whole-body SAR values obtained using the fast REM method and the FDTD simulations for all considered scenarios.

Scenario	Phantoms (M/F)	Positions of phantoms (number of phantoms)	Mean SAR (μW/kg) FDTD	Mean SAR (μW/kg) REM
1	M	05	19.6	38.6
2	M	11	27.1	58.6
3	M	16	18.8	37.7
4	M	19	12.9	31.8
5	M	25	10.4	28.5
6	MFM	07; 09; 18	33.1	48.5
7	MFM	07; 14; 25	18.7	36.4
8	MFM	11; 16; 28	19.7	40.9
9	MFM	11; 19; 24	18.3	41.2
10	MFM	16; 19; 26	13.2	32.4
11	MFMFMF	01; 05; 06; 17; 20; 26	19.2	38.2
12	MFMFMF	02; 08; 13; 16; 22; 27	19.	40.8
13	MFMFMF	04; 06; 10; 11; 15; 28	26.1	48.7
14	MFMFMF	04; 06; 16; 20; 21; 29	16.8	35.6
15	MFMFMF	09; 13; 20; 21; 28; 29	16.1	36.1

REM = room electromagnetics method, FDTD = Finite-difference time-domain
M= male Duke, F = female Ella
Positions are indicated on Figure 1 and separated by a semicolon

Table 1

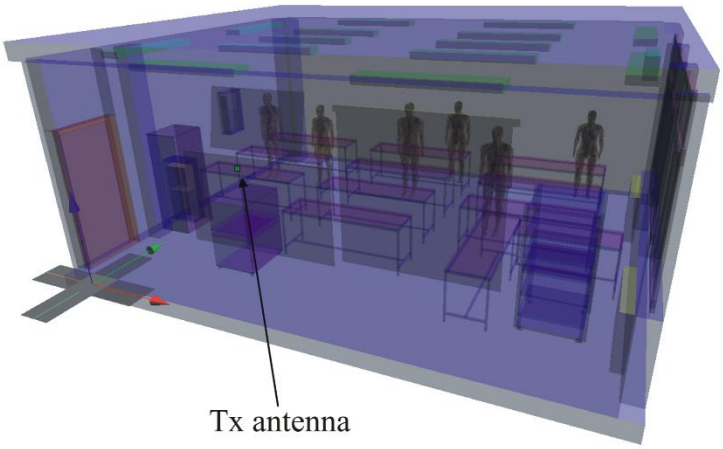
Tx antenna

(a)

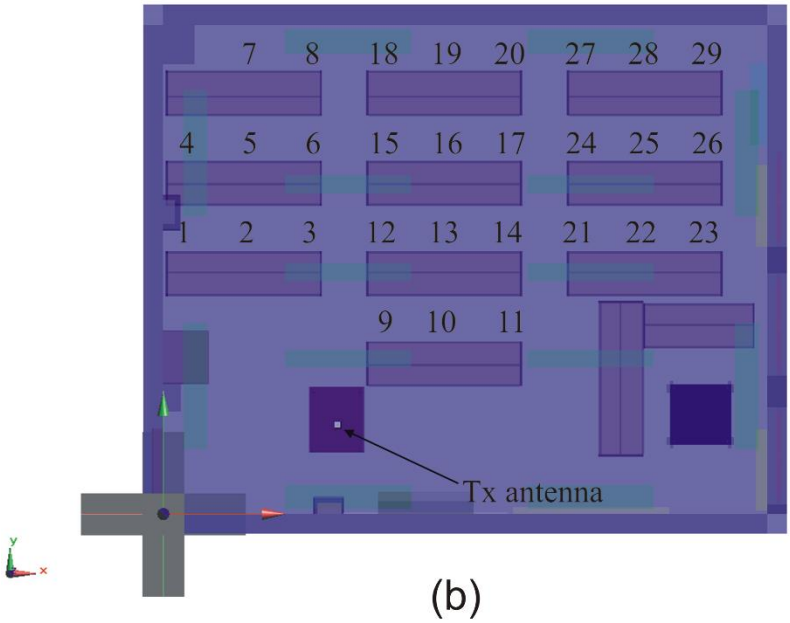
7 8 18 19 20 27 28 29
4 5 6 15 16 17 24 25 26
1 2 3 12 13 14 21 22 23
9 10 11
Tx antenna

(b)

(c)

Figure 1

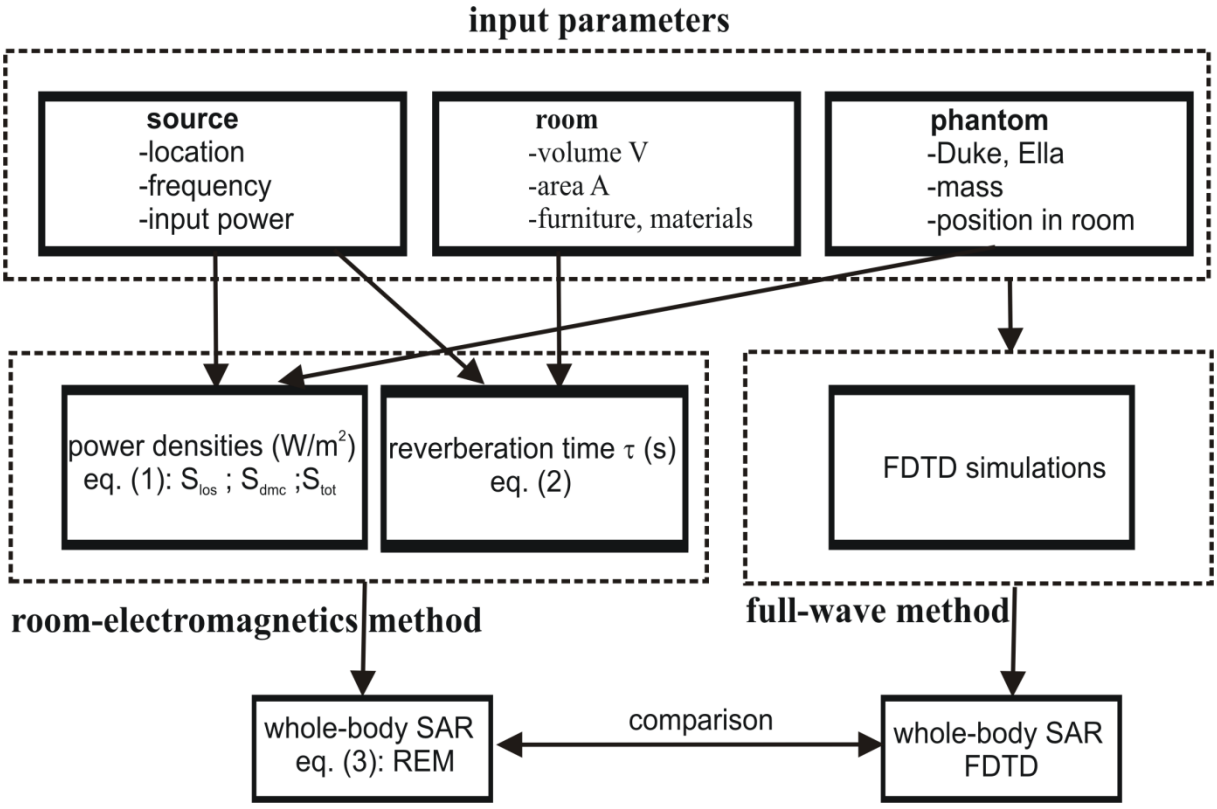
input parameters
source
-location
-frequency
-input power
room
-volume V
-area A
-furniture, materials
phantom
-Duke, Ella
-mass
-position in room
power densities (W/m²)
eq. (1): S_los ; S_dmc ;S_tot
reverberation time τ (s)
eq. (2)
FDTD simulations
room-electromagnetics method
full-wave method
whole-body SAR
eq. (3): REM
comparison
whole-body SAR
FDTD

Figure 2

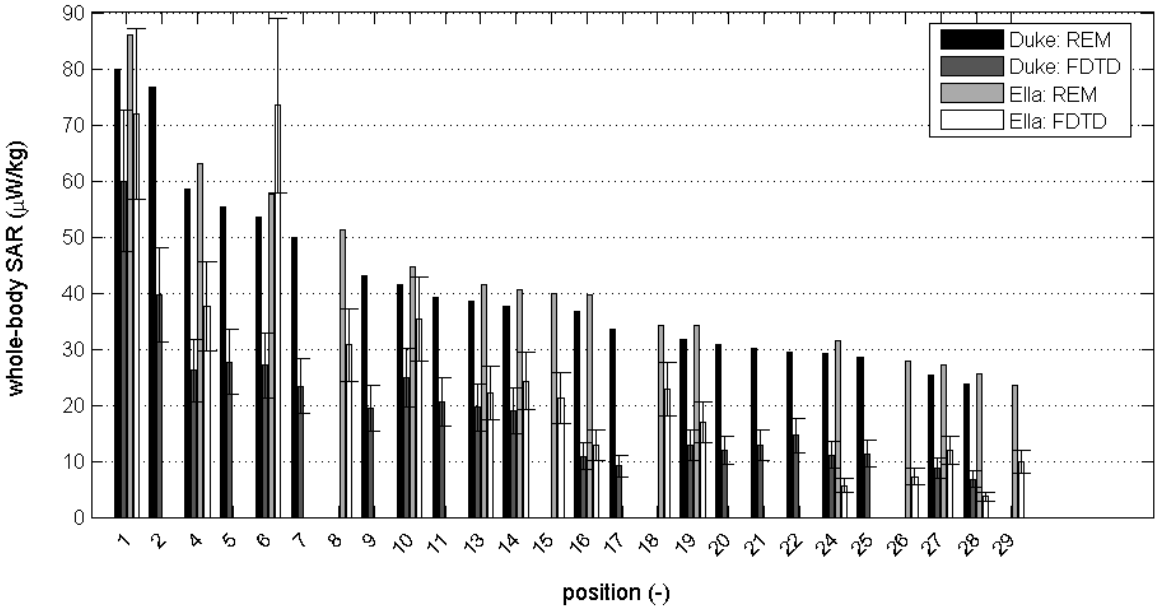
Duke: REM
Duke: FDTD
Ella: REM
Ella: FDTD
whole-body SAR (μW/kg)
position (-)
0
10
20
30
40
50
60
70
80
90
1
2
4
5
6
7
8
9
10
11
13
14
15
16
17
18
19
20
21
22
24
25
26
27
28
29

Figure 3

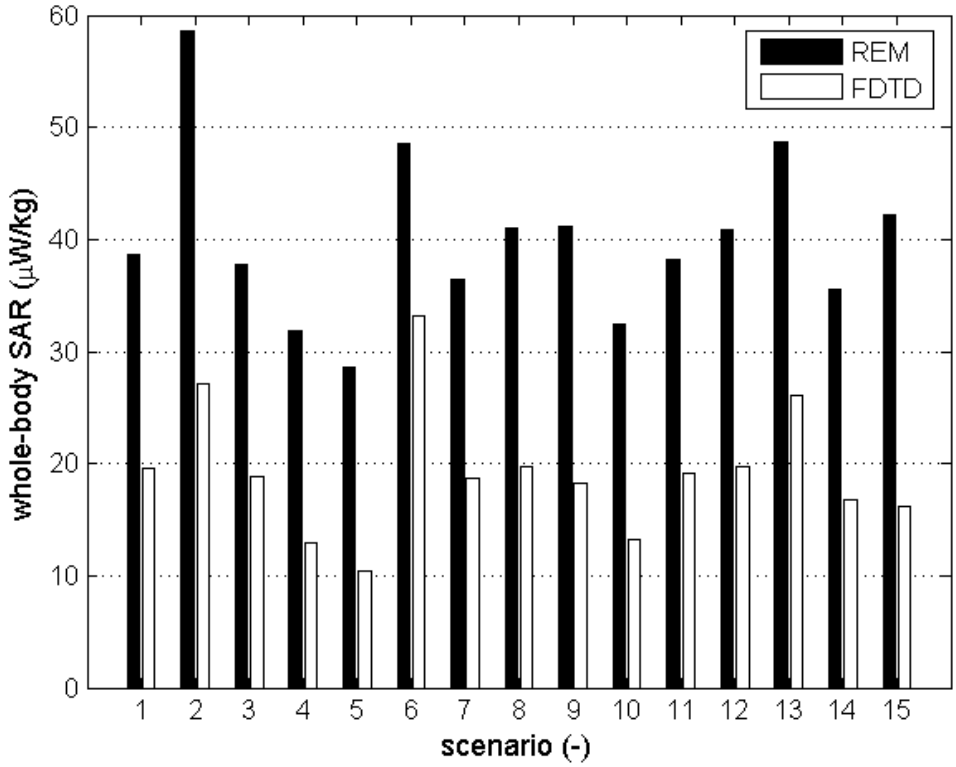
REM
FDTD
whole-body SAR (μW/kg)
scenario (-)
0
10
20
30
40
50
60
1
2
3
4
5
6
7
8
9
10
11
12
13
14
15

Figure 4